Annealing of Ion-Implanted Silicon by a Dense Plasma Focus

J. T. LUE, C.-K. YEH, AND Y.-Y. KUO

Abstract—**The hydrogen ions generated at the open end of the coaxial electrodes of a dense plasma focus (DPF) can be used as a source for the annealing of ion-implanted semiconductors. The versatility of the dense plasma focus bears to its short pinch duration (~ 100 ns), high ion density (~ 10^{19} cm^{-3}), and high thermal energy (~ 10^7 K). Sheet resistance and *I–V* characteristic measurements indicate complete regrowth of the damaged wafers after plasma annealing.**

THE dense plasma focus (DPF) has long been used as a pulsed neutron source since it was initiated by Mather [1], [2] in the U.S. and by Filippov [3] in Russia as part of the controlled thermonuclear fusion program. In this letter, we first report that under certain conditions, the short-pulse high-intensity thermal ion beams can be implemented as a useful tool for annealing of ion-implanted semiconductors. The DPF can generate a very high-density and high-temperature plasma (electron density up to 10^{19} cm^{-3} and electron temperature up to 10^7 K) than other laboratory plasmas. The plasma confinement time is about 100 ns which is very close to the FWHM of *Q*-switched lasers. Current interest on laser annealing has the disadvantage of a small beam profile which requires a scanning of the laser beam for obtaining a uniform annealing area. This inevitably introduces texture structure on the scanned surface [4]. Recently developed light-flash annealing [5]-[7] has a large area of irradiation. However, light-flash annealing on account of its high gas-filling pressure, would exhibit microfracture on the wafer induced by shock waves generated in the tube. Since the fill pressure of the DPF is much lower than that of flash tube (at a ratio of 3-100 torr), the shock wave generated by the plasma is largely diminished and, consequently, with a great improvement on surface morphology and recrystallization effect.

As shown in Fig. 1, the plasma gun is a pair of conducting coaxial cylinders with a ceramic insulator surrounding the lower part of the central anode for guiding the electrical breakdown along the surface. The assembly of the gun must be vacuum tight and the anode at the base plate is bolted tightly to the cathode by 20-mil polyethylene sheets sandwiched in between for preventing relative movement between the anode and cathode during discharge which could crack the ceramic insulator. The material selected for the anode insulator is very critical for successfully obtaining pinch condition [8]. The wafers were attached to a cylindrical rod by vacuum grease which was held at 17 cm from the anode-free end.

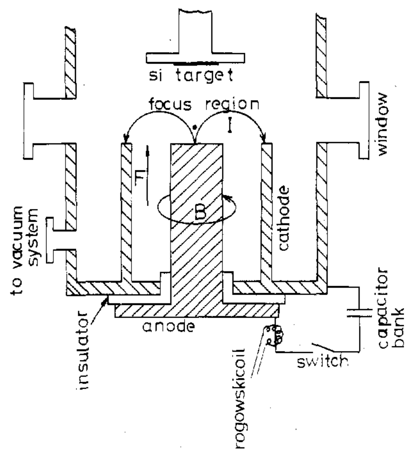

Fig. 1. Schematic diagram of the dense plasma focus device.

Within fractions of a microsecond after the spark gap is ignited, corona breakdown is initiated along the surface of the dielectric insulator in-sleeve of the inner anode. The main discharge current will be developed due to the corona breakdown. The shape of the current sheaths is parabolic and the magnetic inward force is balanced by the gas pressure reflecting from the surface of the central electrode. There is a strong axial force component due to $\hat{J} \times \hat{B}$ force across the annulus thus resulting in a high current sheath near the surface of the central electrode. Plasma pinch will occur at a few centimeters above the plateau of the central anode.

The axisymmetric current wave collapses converting the stored magnetic energy to plasma energy in the focus region. A snowplow model [9] can be applied to account for the ion velocity and pinch time. The implosion velocity of the ions after pinch is estimated to be 10^7 cm/s. Fig. 2 is the current oscillogram of the plasma gun diagnosed by a Rogowski coil. The duration of plasma pinch is much shorter than the whole current discharge time. The electrostatic energy stored in the capacitor (i.e., 20 kV, 19 μf) is dissipitated partly by the spark gap, partly by the resistive heating in the circuit, but predominantly (about 70 percent of $\frac{1}{2}$ C$\cdot$V^2) by converting to the magnetic energy

$$W_k = \int_0^{t_0} \frac{1}{2} I^2 \left.\frac{dL}{dt}\right|_{\text{gun}} \cdot dt \tag{1}$$

for generating the thermal plasma, where $dL/dt|_{\text{gun}}$ is the plasma-inductance change rate. The value of $\dot{L}_{\text{gun}}$ is estimated

Manuscript received August 23, 1983; revised Ocrober 5, 1983. This work was supported in part by the Chinese National Science Council.
J. T. Lue is with the Department of Physics, National Tsing Hua University, Hsin-chu, Taiwan, Republic of China.
C.-K. Yeh and Y.-Y. Kuo are with the Institute of Nuclear Energy Research, Lungtan, Taiwan, Republic of China.

0193-8576/83/1200-0457$01.00 © 1983 IEEE

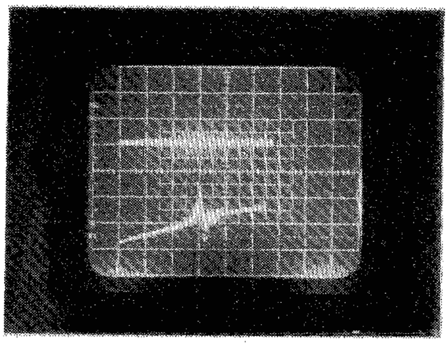

Fig. 2. Oscillograms showing the probing N_2 laser pulse measured by a fast p-i-n diode (upper curve) and dI/dt of the DPF diagnosed by a Rogowski coil (lower curve). The time base of the horizontal line is 40 ns/div giving a pinch duration of about 100 ns.

to be [8]

$$\left.\frac{dL}{dt}\right|_{\text{gun}} = \left[\frac{E^2}{\mu_0 \rho_0}\right]^{1/4} \frac{\mu_0}{2\pi} \ln\left(\frac{b}{a}\right) H/s$$

and

$$E = \frac{V}{\left(\frac{a+b}{2}\right) \ln (a/b)} \tag{2}$$

where ρ_0 is the initial density of the gas and a and b are the radius of the inner and outer electrodes, respectively.

The interferograms of the plasma using the Mach-Zehnder method [10], utilizing a picosecond N_2 UV laser (λ_0 = 3371 Å) is shown in Fig. 3. The electron density n_e at the instant of taking the interferogram can be calculated from the fringe shift $F(r)$ via (1) as given by

$$F(r) = \int_0^l [\mu(\gamma) - 1] \frac{dl}{\lambda_0}, \qquad \mu(\gamma) = 1 - \frac{n_e \lambda_0{}^2 e^2}{2\pi m_e C^2} \tag{3}$$

where l is the plasma thickness presented by the diagnostic light source. The estimated n_e at 10 ns before the onset of peak plasma pinch is $1.6 \times 10^{19}/\text{cm}^3$.

To induce a liquid-solid phase epitaxial growth from a thin amorphous Si layer, a minimum threshold irradiation energy for making the silicon surface to melt is required. If the ions after plasma pinch travel only in the positive half sphere with intensity of triple stronger in the forward direction than in the perpendicular direction [11], [12]. The irradiation energy striking on the wafer at a distance R from the anode can be approximated by

$$E_t = \frac{3}{2} \times \frac{W_k}{\pi R^2}. \tag{4}$$

Since the thermal diffusion length for silicon at temperatures near 600 K within a pulse duration of 100 ns is 182 μm, which is much longer than the hydrogen projected range which is estimated to be below 0.2 μm at 20-keV ion energy, the strong thermal diffusion process [11] can be applied for solving the threshold energy which is inverse proportional to the square root of the pulse duration. If the ion energy during pinch time is much higher than that at other instants of current discharge, the annealing effect can be assumed to be essentially performed during pinch time. To check the threshold energy $E_L{}^T$ as estimated from (4), we can solve the diffusion equation analytically by assuming the thermal conductivity K and specific heat are constant during annealing. We find [11]

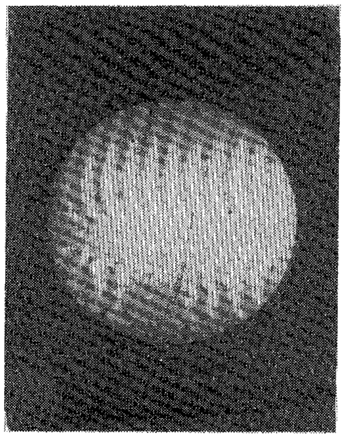

Fig. 3. Interferograms of the DPF using Mach-Zehnder method taken at 10 ns before peak plasma pinch.

$$E_L{}^T = 2T_M K_s \sqrt{\frac{\tau_p}{\pi \kappa_s}} \Bigg/ \left(1 + \frac{2}{\pi} \int_0^\infty \frac{e^{-\frac{3}{4}\pi z^2} dz}{1 + z^4}\right) \tag{5}$$

where T_M is the melting temperature, K_s and κ_s are the thermal conductivity and thermal diffusivity of silicon, respectively, and τ_p is the pulse duration assuming a sinusoidal input energy. The threshold energy $E_L{}^T$ = 0.477 J/cm^2 for τ_p = 100 ns is very close to the value E_t = 0.49 J/cm^2, as estimated from (4) by the measurement of discharge current I.

The silicon samples ([111], 1 ~ 10 Ω·cm, n-type) are implanted by 150-keV $BF_2{}^+$ ions with fluences ranging from 10^{14} to 10^{16} ions/cm^2. The annealing results can be checked readily by a four-point probe, since sheet resistance reflects the impurity activation and lattice perfection. Table I shows that the sheet resistance of the DPF-annealed wafers depend greatly on the fill pressure. At higher fill pressure ($p > 8$ torr), the ion energy decreases due to the smallness of mean-free path with a consequence of incomplete annealing effect. The plasma pinch behaves most strongly near 3 torr resulting in complete annealing.

The I-V plot as shown in Fig. 4 reveals that annealing at 0.49 J/cm^2 forms an ideal diode. With incomplete annealing (at high fill presure or low bank energy), the cut-in voltage and the dynamic resistance of the diode both increase indicating the imperfect regrowth of the implanted wafer. Surface morphology as checked by an optical microscope indicates that no slip-trace has been found even for high-dose implanted wafers with complete DPF annealing [13]. Except at fill pressure below 3 torr, the surface erosion due to ion sputtering is catastrophic.

TABLE I
SHEET RESISTANCE OF DPF-ANNEALED WAFERS WITH THE SAME SPECIFICATION AS GIVING IN FIG. 4 AT VARIOUS GAS-FILLING PRESSURES

Fill pressure of the DPF (torr)	10	8	6	5	3	2	1
Sheet resistance (Ω/□)	3195	2385	731	387	<74.7	9	<50
Irradiation energy density (J/cm^2)	0.36	0.38	0.41	0.43	0.49	0.54	0.64

Note: The irradiation energy is evaluated by first measure the peak discharge current $I_0 = \pi c V/T$, where T is the period of current oscillation which is 9 sec in this circuit. The plasma pinch occurs almost at $t_0 = T/4$ for a matched circuit, so that W_K can be readily calculated from Eq. (1). The irradiation energy is inverse proportional to $(\rho_0)^{1/4}$.

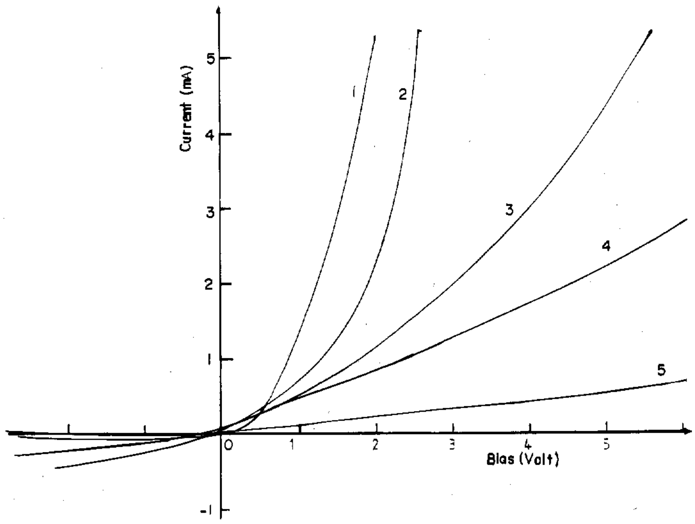

Fig. 4. *I-V* characteristic of DPF annealing of 150-keV BF_2^+ implanted Si wafers at a dose of 5×10^{15} cm^{-2} at a capacitor-supplying voltage of 19.5-kV and a wafer-to-anode distance of 15 cm. Different curves showing different DPF filling pressures: 1) $P_{H_2} = 2$ torr; 2) 3 torr; 3) 900°C 30-min furnace annealing; 4) 5 torr; 5) 8 torr.

The DPF annealing has advantages of having a low-cost large-beam profile, and less microcrack damage to the wafer by shock wave. The drawback is that the energy released by the DPF is not very reliable, since the pinch condition depends on the history of the dielectric insulator and on the impedance jitter of the spark gap. The plasma pinch will be stable only after some shots of the tube. If a proper dielectric material can be chosen and a high peak current thyratron can replace the spark gap, the result will be more repeatable.

REFERENCES

[1] J. W. Mather, *Phys. Fluids*, Suppl., vol. 7, p. 28, 1964.
[2] ——, *Phys. Fluids*, vol. 8, p. 366, 1965.
[3] N. V. Filippov, T. I. Filippov, and V. P. Vinigradov, *Nucl. Fusion*, Suppl., vol. 2, p. 73, 1962.
[4] H. J. Leamy, G. A. Rozgonyi, and T. T. Sheng, *Appl. Phys. Lett.*, vol. 32, p. 535, 1978.
[5] A. Usami, N. Yoshida, and Y. Inoue, *IEEE Electron Device Lett.*, vol. EDL-4, p. 166, 1983.
[6] G. Bentini, L. Correra, R. Galoni, L. Pedulli, J. C. Muller, A. Mesli, M. Hage-Ali, and P. Siffert, "Unanalyzed ion implanation procedure with incoherent light scanning annealing for silicon solar cell manufacturing," in *Proc. 16th IEEE Photo-Voltaic Specialist Conf.*, 1982, p. 295.
[7] J. T. Lue, *Int. J. Vacuum*, vol. 32, p. 713, 1982.
[8] K. F. Yeung, Ph.D. dissertation, Dep. Nucl. Eng., Univ. of Illinois, Urbana-Champaign, IL, 1976.
[9] J. T. Lue and J. M. Lian, *Appl. Phys. Lett.*, vol. 31, p. 798, 1977.
[10] F. C. Jahoda and G. A. Sawyer, *Methods of Experimental Physics*, vol. 9, part B, H. R. Griem and R. H. Lovbery, Eds. New York: Academic Press, 1970, p. 1.
[11] J. T. Lue and C. C. Chao, *J. Appl. Phys.*, vol. 53, p. 984, 1982.
[12] A. Bernard, P. Cloth, H. Conrads, A. Coudeville, G. Goulan, A. Jelas, C. H. Maisennier, and J. P. Ragen, *Nucl. Instrum. Methods*, vol. 145, p. 191, 1977.
[13] J. T. Lue, L. C. Cheng, and L. Z. Lu, *Solid-State Electron.*, vol. 25, p. 559, 1982.